Modeling of permanent magnets: Interpretation of parameters obtained from the Jiles–Atherton hysteresis model

L. H. Lewis, J. Gao, D. C. Jiles, and D. O. Welch

Citation: Journal of Applied Physics **79**, 6470 (1996); doi: 10.1063/1.361975
View online: http://dx.doi.org/10.1063/1.361975
View Table of Contents: http://scitation.aip.org/content/aip/journal/jap/79/8?ver=pdfcov
Published by the AIP Publishing

Modeling of permanent magnets: Interpretation of parameters obtained from the Jiles–Atherton hysteresis model

L. H. Lewis
Department of Applied Science, Brookhaven National Laboratory, Upton, New York 11973

J. Gao and D. C. Jiles
Ames Laboratory, Iowa State University, Ames, Iowa 50011

D. O. Welch
Department of Applied Science, Brookhaven National Laboratory, Upton, New York 11973

The Jiles–Atherton theory is based on considerations of the dependence of energy dissipation within a magnetic material resulting from changes in its magnetization. The algorithm based on the theory yields five computed model parameters, M_S, a, α, k, and c, which represent the saturation magnetization, the effective domain density, the mean exchange coupling between the effective domains, the flexibility of domain walls and energy-dissipative features in the microstructure, respectively. Model parameters were calculated from the algorithm and linked with the physical attributes of a set of three related melt-quenched permanent magnets based on the $Nd_2Fe_{14}B$ composition. Measured magnetic parameters were used as inputs into the model to reproduce the experimental hysteresis curves. The results show that two of the calculated parameters, the saturation magnetization M_S and the effective coercivity k, agree well with their directly determined analogs. The calculated a and α parameters provide support for the concept of increased intergranular exchange coupling upon die upsetting, and decreased intergranular exchange coupling with the addition of gallium. © *1996 American Institute of Physics.* [S0021-8979(96)27608-2]

I. INTRODUCTION

The various relationships between structure and properties in permanent magnet materials are usually explored by experimental methods. With a few notable exceptions,[1,2] these relationships have not yet been extensively explored by theoretical modeling. We present here an inaugural investigation of the results which link model parameters calculated from an algorithm based on the Jiles–Atherton theory[3] with the physical attributes of a set of three related melt-quenched and thermomechanically treated permanent magnets based on the $Nd_2Fe_{14}B$ composition. Interpretations of the information thus yielded provides substantial insight into the hypothesized reversal mechanisms and internal coupling found in these magnets.

II. THE HYSTERESIS MODEL ALGORITHM

The Jiles–Atherton model[4–6] of hysteresis is based on consideration of the dependence of energy dissipation on change in magnetization, the principal cause of hysteresis in multidomain specimens. Consideration of the underlying mechanisms has produced two differential equations which represent the irreversible differential susceptibility and reversible differential susceptibility. The solution of these differential equations leads to a normal sigmoidal-shaped hysteresis curve, when combined with an appropriate choice of function for the anhysteretic magnetization. The algorithm requires input of nine experimentally measured parameters: The coercivity $H_{\rm ci}$, the remanence B_R, the initial normal susceptibility $\chi'_{\rm in}$, the initial anhysteretic susceptibility $\chi'_{\rm an}$, the differential susceptibility at the coercive point $\chi'_{H_{\rm ci}}$, the differential susceptibility at remanence χ'_{B_R} and the coordinates (H_m, M_m) of the loop tip, as well as the differential susceptibility of the initial magnetization curve at the loop tip, χ'_m.[4] The algorithm yields five computed model parameters, M_S, a, k, α, and c. The physical interpretation of these five model parameters is given as follows.

M_S is the saturation magnetization of the material, and thus the validity of this parameter is very easy to check, either by experimental means or by obtaining the data from references. The units of M_S are A/m or emu/cc.

The a parameter is sometimes referred to as the ''effective domain density.'' The model parameter a is derived from an analogy to the Langevin expression[7] for the anhysteretic magnetization $M_{\rm an}$ as a function of both temperature T and field H for a paramagnet:

$$M_{\rm an}(H,T) = M_S \times [\coth(H/a) - (a/H)], \tag{1}$$

where $a = k_B T/(\mu_0 \langle m \rangle)$; M_S is the saturation magnetization and k_B is Boltzmann's constant. However, in the Jiles–Atherton theory, the spin entity $\langle m \rangle$ is not an atomic magnetic moment $m = n\mu_B$, where μ_B is the Bohr magneton, as in the original Langevin expression. Rather, it represents the moment from a mesoscopic collections of spins that we refer to as an ''effective domain;'' each ''effective domain'' possesses a collective magnetic moment $\langle m \rangle$. These effective domain entities may or may not correspond to actual magnetic domains; the units of a are in A/m or Oe.

k gives a measure of the quasistatic energy dissipation via the expression $k = (1/\mu_0) \times dE/dM$, with μ_0 as the permeability of free space and dE/dM the change in energy per change in magnetization. In the case of a material for which the coercivity is controlled by domain-wall pinning, this expression is related to effect of pinning sites on the progress

 0021-8979/96/79(8)/6470/3/$10.00

TABLE I. Sample descriptions and model parameter results calculated from the Jiles–Atherton algorithm.

Sample identification	Bulk composition	Processing	M_S (emu/cc)	a(Oe)	k(Oe)	α	c
HP1553	$Nd_{13.75}Fe_{80.25}B_6$	Hot pressed (MQ-2)	1080	13920	8825	3.168	0.885
DU1418	$Nd_{13.75}Fe_{80.25}B_6$	Die upset (MQ-3)	1000	1247	4100	0.742	0.485
DU2162	$[Nd_{13}(Fe_{0.95}Co_{0.05})_{81}B_6]_{0.996}Ga_{0.004}$	Die upset (MQ-3)	1100	3748	8246	1.472	0.885

of the hysteresis. In soft materials k is approximately equal to the coercivity H_{ci}; in hard materials it is equal to a modified form of the coercivity:[8]

$$k=\frac{M_{an}(H_c)}{1-c}\times\left\{\alpha+\frac{1}{\chi'_{max}-\left(\frac{c}{1-c}\right)\times\frac{dM_{an}(H_c)}{dH}}\right\}. \qquad (2)$$

M_{an} is the anhysteretic magnetization as defined in Eq. (1); the units of k are A/m or Oe. An explicit expression for k has not been derived for the case where the coercivity is controlled by the nucleation of reversed domains; however, in general it is to be expected that k should increase when the density of domain reversal sites decreases.

α is a dimensionless quantity that describes the mean interaction field experienced by the effective domains, in a manner completely analogous to the Weiss molecular field: $H_{ex}=\alpha M$, where M is the magnetization.

The dimensionless model parameter c gives a measure of the relative magnitude of the reversible magnetization contribution to the total magnetization, and is defined by the expression $\chi'_{in}=c\chi'_{an}$.

III. RESULTS

The hysteresis loops that provided the experimental inputs to the model algorithm were obtained from three related, melt-quenched and thermomechanically processed magnets obtained from General Motors R. & D. Center. The bulk compositions of the magnets are given in Table I, along with some processing details. The samples were measured at $T=350$ K using a Quantum Design MPMS SQUID magnetometer with the furnace insert. The sample measurement configuration and subsequent data analysis is described in detail in Ref. 9.

Iterations of the parameter-determination algorithm produced the results presented in Table I. In general, the fits between the calculated and the experimental hysteresis loops were very good, being in error by less than 5% of the whole of the hysteresis curve. Figures 1(a)–(c) show the calculated hysteresis loops superimposed upon the measured loops. The calculated saturation magnetization values, M_S, agree well with the experimentally determined ones. The model parameters, a, k, and α, show very interesting variations from sample to sample, especially as the sample HP1553 was die upset to become DU1418. The parameters a and α, representative of the density of ''effective domains'' and the operative interdomain coupling, respectively, decreased sharply with die upsetting. These quantities recovered somewhat in the sample DU2162, doped with cobalt and gallium. The value of the k parameter, illustrating the average pinning

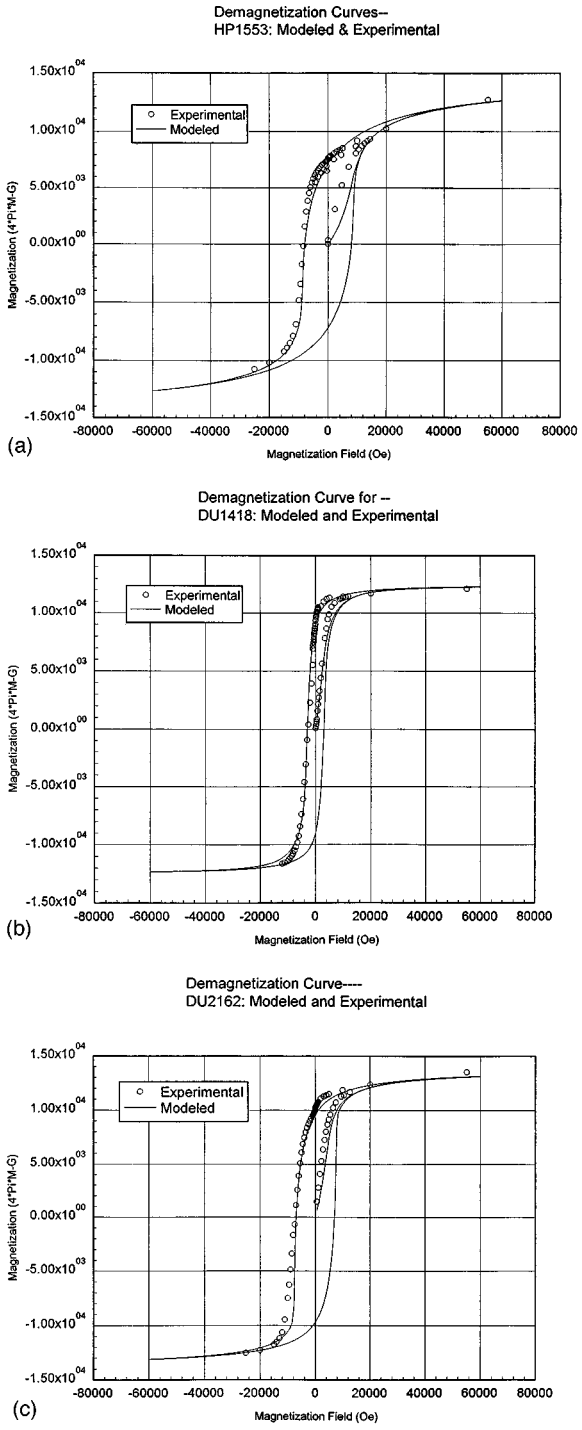

FIG. 1. (a) Hysteresis loops for sample HP1553 ($Nd_{13.75}Fe_{80.25}B_6$), modeled and experimental. (b) Hysteresis loops for sample DU1418 ($Nd_{13.75}Fe_{80.25}B_6$), modeled and experimental. (c) Hysteresis loops for sample DU2162 ($[Nd_{13}(Fe_{0.95}Co_{0.05})_{81}B_6]_{0.996}Ga_{0.004}$), modeled and experimental.

strength of the inhomogeneities in the materials, is roughly the same in HP1553 and DU2162, but is approximately half that value in DU1418.

IV. DISCUSSION

In order to lend physical insight to the calculated model parameters, a review of recent microstructural and magnetic characterization of the samples is necessary. The process of die upsetting a hot-pressed sample introduces drastic changes within the microstructure. A melt-quenched and hot-pressed sample typically consists of a dense collection of mostly equiaxed grains with dimensions on the order of 100 nm. Preliminary transmission electron microscopy (TEM) investigations performed at Brookhaven National Laboratory indicate that the grain size dispersion of HP1553 is small. Some researchers have found an additional phase in the microstructure, identified by electron diffraction as $Nd_5Fe_2B_5$.[10] An intergranular phase has also been identified at the grain boundaries[11] of hot-pressed samples and is reported to have a composition close to the eutectic composition in the Nd–Fe binary system, $Nd_{70}Fe_{30}$.

With die upsetting, the grains not only increase in size, but they become highly anisotropic. The die-upset structure consists of platelet-shaped grains of the 2–14–1 phase stacked along the press direction, the 2–14–1 tetragonal *c* axis. A thin intergranular phase has also been identified in these magnets, but the nature and composition of this phase is in dispute. Mishra *et al.*[11,12] report that the intergranular phase is crystalline (fcc), seems to uniformly coat all grains, and has a composition close to $Nd_{70}Fe_{30}$. Recent results, obtained with high resolution TEM methods[9,13] using a nominal 5 Å probe size, have demonstrated the existence of an amorphous grain boundary phase present in DU1418 and a related sample, die-upset PrFeB. Based on a sampling of 30 grain boundaries, the phase clearly shows an enrichment of iron in the grain boundary region relative to the grain itself; it does not evenly wet all surfaces of the deformed 2–14–1 main phase particles, but is found mainly on those boundaries parallel to the *c* axis.

Magnetic studies performed on DU1418 at elevated temperatures[9] show a linear development of both remanence and coercivity with applied field after thermal demagnetization, consistent with the phenomena of nucleation of reverse domains. The coercivity and remanence in HP1553 and DU2162 also show this same linear dependence. It has been postulated that the iron-rich grain boundary phase may act as a reverse grain nucleation site of lowered anisotropy, as well as providing a means to exchange couple the constituent grains.[9]

The above results lend interpretation to the calculated model parameters. The decrease in the *a* parameter from the relatively high value of 13920 Oe in HP1553 to the low value of 1247 Oe in DU1418 represents a decrease in the density of effective domains, as described in Sec. II. This decrease is consistent with a change in the microstructure that promotes exchange coupling among the grains in the die-upset sample, as would be expected if a significant portion of intergranular phase changed in composition from rare-earth rich to iron rich. The increase of the *a* parameter in DU2162, the sample doped with both cobalt and gallium, relative to that of DU1418, is consistent with a certain amount of exchange decoupling between the grains that serves to produce a greater density of ''effective domains.'' Many researchers[14–17] believe that the addition of gallium to 2–14–1-based magnets segregates to the grain boundary phase; such a segregation would be expected to decrease the intergranular coupling by diluting the magnetic properties of the intergranular phase. Consistent with the above discussion, the variation of calculated *k* parameters can be ascribed to the difficulty in the nucleation of reversed grains. This difficulty may be traced to a dearth of Fe-rich, low-anisotropy rich regions in the microstructures of HP1553 and DU2162 of the proper dimensions to allow nucleation of reverse domains upon the application of a magnetizing field to a thermally demagnetized sample.

The calculated α parameters indicate that the coupling between the ''effective domains'' in HP1553 is somewhat stronger than that found in DU2162, and is much stronger than that found in DU1418. Such a result may be attributed to differences in the chemistry, thickness and occurrence of the iron poor intergranular and triple-point junction phases found in each material; the iron-rich intergranular phases presumably exist within the volume of the ''effective domain'' and do not contribute to α. Work is presently underway to thoroughly characterize the grain boundary phases in these materials using advanced TEM methods.

ACKNOWLEDGMENTS

We are grateful to C. D. Fuerst of General Motors R. & D. Center for providing us with samples and for helpful discussions. This research was sponsored by U.S. DOE, Laboratory Directed Research and Development Program, Contract No. DE-AC02-76CH00016.

[1] F. Preisach, Z. Phys. **94**, 277 (1935).
[2] E. C. Stoner and E. P. Wohlfarth, Philos. Trans. R. Soc. London, Ser. A **240**, 599 (1948).
[3] D. C. Jiles and D. L. Atherton, J. Magn. Magn. Mater. **61**, 48 (1986).
[4] D. C. Jiles, J. B. Thoelke, and M. K. Devine, IEEE Trans. Magn. **28**, 27 (1992).
[5] D. C. Jiles, J. Appl. Phys. **76**, 5849 (1994).
[6] D. C. Jiles and M. K. Devine, J. Magn. Magn. Mater. **140**, 1881 (1995).
[7] S. Chikazumi, *Physics of Magnetism* (Krieger, Malabar, FL, 1964).
[8] D. C. Jiles and J. B. Thoelke, IEEE Trans. Magn. **25**, 3928 (1989).
[9] L. Henderson Lewis, Y. Zhu, and D. O. Welch, J. Appl. Phys. **76**, 6235 (1994).
[10] T.-Y. Chu, L. Rabenberg, and R. K. Mishra, J. Appl. Phys. **69**, 6046 (1991).
[11] R. K. Mishra, J. Appl. Phys. **62**, 967 (1987).
[12] R. K. Mishra, T.-Y. Chu, and L. K. Rabenberg, J. Magn. Magn. Mater. **84**, 88 (1990).
[13] Y. Zhu, J. Tafto, L. H. Lewis, and D. O. Welch, Philos. Mag. Lett. **71**, 297 (1995).
[14] V. Panchanathan and J. J. Croat, IEEE Trans. Magn. **25**, 4111 (1989).
[15] M. Tokunaga, Y. Nozawa, K. Iwasaki, M. Endoh, S. Tanigawa, and H. Harada, IEEE Trans. Magn. **25**, 3561 (1989).
[16] C. D. Fuerst and E. G. Brewer, J. Appl. Phys. **73**, 5751 (1993).
[17] I. Ahmad, H. A. Davies, and R. A. Buckley, Mater. Lett. **20**, 139 (1994).